XLVI CILAMCE
VITÓRIA - ES - BRAZIL - 2025
XLVI IBERO-LATIN AMERICAN CONGRESS ON COMPUTATIONAL METHODS IN ENGENEERING

Numerical benchmarking of Stabilized Finite Element Methods applied to the Population Balance Equation for modeling crystal size distributions

Andrés M. Nieves Chacón[1], Regina C. Almeida[2], Renato S. Silva[2]

[1]*Programa de Pós-graduação em Modelagem Computacional do Laboratório Nacional de Computação Científica*
andresmn@posgrad.lncc.br
[2]*Laboratório Nacional de Computação Científica*
Av. Getúlio Vargas - 333, CEP 25651-075, Petrópolis/RJ, Brazil
rssr@lncc.br, rcca@lncc.br

Abstract. Crystallization fouling is a prevalent phenomenon observed in heat exchangers, involving the accumulation of crystals on heat transfer surfaces. This buildup reduces thermal efficiency and raises operational costs in industrial systems. The net fouling rate depends on the balance between deposition and removal mechanisms. Deposition occurs when crystals, transported by diffusion from high to low-concentration regions, adhere to surfaces at a reaction-specific rate. In contrast, the removal process is driven by hydrodynamic forces and shear stresses acting on the deposited layer. The removal process is highly dependent on crystal size, as changes in size alter key mechanical properties (e.g., material strength, Young's modulus, and hardness) and thermophysical properties (e.g., thermal conductivity and density). Consequently, accurately characterizing the crystal size distribution within the fouling layer is essential. The population balance equation (PBE) is widely employed for this purpose, providing a mechanistic framework to model evolving particle sizes and their impact on fouling dynamics. To solve the PBE, different numerical approaches have been proposed, including weighted residual methods. In this paper, we investigate the performance of some Stabilized Finite Element Methods (SFEMs) applied to the PBE for modeling the growth, aggregation, and nucleation processes involved in crystallization fouling. The stabilized formulations include the Streamline Upwind Petrov-Galerkin (SUPG) and the Galerkin Least Squares (GLS) methods, utilizing various stabilization parameters. The numerical behavior of these SFEMs is assessed based on their ability to reproduce expected physical behavior, providing insights for future model developments.

Keywords: Stabilized Finite Element Methods, Population Balance Equation, Crystallization fouling

1 Introduction

Heat exchangers are essential devices that transfer heat between fluids with applications in various industries, including power generation, oil and gas, petrochemicals, and food processing. However, fouling poses significant challenges in such equipment, as it increases thermal resistance, reduces heat exchanger efficiency, and leads to higher energy consumption and maintenance costs [1]. Crystallization is among the most common categories of fouling, along with chemical reaction, biological, and corrosion fouling phenomena [2]. Regardless of the fouling type, according to Epstein [3], the fouling process typically involves five key stages: (a) initiation, (b) transport, (c) attachment, (d) removal, and (e) aging. During the final stage of fouling, the deposited material undergoes aging, which alters its fundamental properties. For example, a population of $CaCO_3$ crystals evolves through nucleation, growth, and agglomeration, forming crystals with a broad size distribution. Consequently, crystal size emerges as a critical parameter, since aging influences both thermophysical properties (e.g., thermal conductivity, density) and mechanical properties (e.g., crystal strength, tensile behavior). The aging process of crystals significantly affects their removal behavior, as changes in mechanical properties directly impact detachment potential. For instance, if thermal stresses exceed the material's strength, crystalline deposits may undergo mechanical failure and a subsequent break-off process [4]. The phenomenon is particularly relevant in fouling layers, impacting their stability and overall dynamics.

In our initial analysis, we characterize the crystal size distribution through the solution of the population balance equation (PBE). This integro-differential hyperbolic equation presents significant numerical complexity, particularly due to the formation of regions with steep solution gradients. To overcome these computational challenges, various specialized numerical approaches for PBE solution have been developed [5]. The Classical

Galerkin Finite Element Method often suffer from numerical instabilities, leading to spurious oscillations in solutions. To mitigate these issues, stabilized Petrov-Galerkin methods such as the Streamline Upwind Petrov–Galerkin (SUPG) [6] and the Galerkin Least Squares (GLS) [7] methods can be applied. The stability and accuracy of these methods critically depend on the optimal selection of stabilization parameters, which are typically derived from local mesh and crystal growth rate conditions.

This study systematically evaluates the performance of both SUPG and GLS methods by examining different stabilization parameter schemes from the literature. Our objective is to assess their ability to eliminate numerical artifacts while preserving physically realistic solutions, ultimately providing guidelines for robust model implementation in crystallization fouling simulations.

2 The Population Balance Equation

The PBE characterizes how a population of solid or fluid particles is distributed based on an intrinsic property such as mass, volume, length, porosity, among others. Focusing on any of these properties provides meaningful descriptions of particle composition. The PBE is used to analyze the evolution of particle populations driven by growth, aggregation, and nucleation phenomena, and applies to a wide range of engineering fields, including crystallization, cell dynamics, polymerization, and mixing processes [8]. The general form of the PBE is given by

$$\frac{\partial f(x,t)}{\partial t} + \frac{\partial [g(x,t)f(x,t)]}{\partial x} = \mathcal{A}_B(x,t) - \mathcal{A}_D(x,t)f(x,t) + \mathcal{N}(x,t), \quad \text{in} \quad \Omega \times T \tag{1}$$

$$f(x,0) = f_0(x), \quad x \in \overline{\Omega}. \tag{1a}$$

Here, Ω and T respectively represent the spatial and temporal domains such that $\Omega = (x_{\min}, x_{\max})$ and $T = (0, t_\infty]$. In Eq. (1), $f(x,t)$ denotes the number density function of crystals with volume x at time t. The main features of this equation are highlighted as follows: ***(i)*** Eq. (1a) defines the initial number density distribution, ***(ii)*** the growth function, denoted by $g(x,t)$, defines the rate at which crystals increase in size over time. In the PBE, $g(x,t)$ is associated with the convection term, representing the transport of particles along the crystal volume domain due to growth, ***(iii)*** the function $\mathcal{A}_B(x,t)$ denotes the birth rate of crystals of volume x, resulting from the aggregation of two crystals with volumes u and $x-u$, where $u \in \Omega$. Conversely, $\mathcal{A}_D(x,t)$ represents the death rate of crystals of volume x due to their aggregation with crystals of smaller volumes, thereby contributing to the formation of larger crystals with volume $x+u$. These terms are defined as follows

$$\mathcal{A}_B(x,t) = \frac{1}{2}\int_0^x \beta(x-u,u,t)f(x-u,t)f(u,t)\,du), \tag{2}$$

$$\mathcal{A}_D(x,t) = \left(\int_0^\infty \beta(x,u,t)f(u,t)\,du\right). \tag{3}$$

Here, $\beta(x,u,t)$ denotes the aggregation kernel, which quantifies the frequency at which crystals of volumes x and u collide and adhere to form a larger crystal, ***(iv)*** the function $\mathcal{N}(x,t)$ represents the nucleation term, which accounts for the formation of new crystals of sizes $x \geq x_{\min}$ at time t and ***(v)*** the functions $\mathcal{A}_B(x,t)$ and $\mathcal{N}(x,t)$ act as source terms, while $\mathcal{A}_D(x,t)$ plays the role of an explicit reaction coefficient.

3 Numerical approximation

Let the time domain $(0, t_\infty]$ be divided into n constant time steps $\Delta t = t_\infty/n$. Consider a finite element partition $\mathcal{K}^h$ composed of one dimensional linear elements Ω_e such that $\overline{\Omega} = \bigcup_{e=1}^{N_e} \overline{\Omega_e}$, $\quad \bigcap_{e=1}^{N_e} \Omega_e = \emptyset$, where N_e is the total number of elements in $\mathcal{K}^h$. Denoting $\langle \cdot, \cdot \rangle$ as the L^2-inner product over Ω, let $\mathcal{V}^h \subset \mathcal{V} \equiv H^1(\Omega)$ be finite element spaces. For each time step, $f^h \in \mathcal{V}^h$ is the Galerkin solution to Eq.(1) if:

$$\left\langle \frac{\partial f^h}{\partial t}, v^h \right\rangle + G(f^h, v^h) = F_G(v^h), \quad \left\langle f^h - f_0, v^h \right\rangle = 0, \quad \forall v^h \in \mathcal{V}^h, \tag{4}$$

where $G(f^h, v^h)$ and $F_G(v^h)$ respectively correspond to the bilinear and linear forms given by

$$G(f^h, v^h) = \left\langle g_0 \frac{\partial f^h}{\partial x}, v^h \right\rangle + \left\langle \mathcal{A}_D^h, v^h \right\rangle \quad \text{and} \quad F_G(v^h) = \left\langle \mathcal{A}_B^h, v^h \right\rangle + \left\langle \mathcal{N}^h, v^h \right\rangle. \tag{5}$$

By defining the differential operator as

$$\mathcal{L}(\cdot) = \frac{\partial(\cdot)}{\partial t} + g_0 \frac{\partial(\cdot)}{\partial x} + \mathcal{A}_D(\cdot), \quad \text{in } \Omega_e, \tag{6}$$

and adding a perturbation term p_e^h to the usual Galerkin weighted function v^h, we derive the following general Petrov–Galerkin formulation:

$$\left\langle \frac{\partial f^h}{\partial t}, v \right\rangle + G(f^h, v^h) + \sum_{e=1}^{N_e} \left\langle \mathcal{L}(f^h), p_e^h \right\rangle_{\Omega_e} = F_G(v^h) + \sum_{e=1}^{N_e} \left\langle \mathcal{A}_B + \mathcal{N}, p_e^h \right\rangle_{\Omega_e}, \quad \forall v^h \in \mathcal{V}^h. \tag{7}$$

3.1 The SUPG and the GLS methods

The SUPG and GLS methods represent specialized Petrov-Galerkin formulations that incorporate consistently designed perturbation terms. In the SUPG method [7], stabilization is achieved through a streamline-oriented perturbation that aligns with the growth direction in the population balance equation (PBE). The perturbation term takes the form:

$$p_e^h \to p_{SUPG}^h = \tau_e g_0 \frac{\partial v^h}{\partial x}, \quad \forall e = \{1, ..., N_e\}, \tag{8}$$

in which τ_e represents the element-wise stabilization parameter to be defined later. The GLS method [7] employs an alternative stabilization approach, applying the differential operator $\mathcal{L}$ to the weighting function v^h. This yields a perturbation term of the form:

$$p_e^h \to p_{GLS}^h = \tau_e \mathcal{L}(v^h), \quad \forall e = \{1, ..., N_e\}. \tag{9}$$

We conduct a numerical comparison of the stability and accuracy performance for the aforementioned stabilized methods using the parameter sets documented in Table 1. For the advection-dominated regimes under investigation, these stabilization parameters incorporate three key physical scales: ***(i)*** the characteristic element size h_e, ***(ii)*** the temporal discretization scale Δt, and ***(iii)*** the reaction coefficient $\mathcal{A}_D$. Each parameter variant in Table 1 has been formulated to target specific aspects of the system dynamics, as detailed in the accompanying description.

Table 1. Stabilization parameters used in the Petrov-Galerkin formulations

Reference	Stabilization parameter	Description
Hughes et al. [7]	$\tau_e = (\xi/\sqrt{15})(h_e/g_0)$	This parameter is proposed for the transient one-dimensional case, where $\xi = 1$ for pure convection scenario.
Tezduyar and Osawa [9]	$\tau_e = \left[(h_e/2g_0)^{-2} + (\Delta t/2)^{-2}\right]^{-1/2}$	This parameter comprises two components: the first accounts for convection and the second one for temporal effects.
Codina [10]	$\tau_e = [(2g_0/h_e) + \mathcal{A}_D]^{-1}$	Although this parameter does not include a contribution from the temporal term, it incorporates the reaction coefficient $\mathcal{A}_D$.

4 Computational implementation and the performance evaluation strategy

The computational implementation of the methods described in the previous subsections is carried out using the Python language and considering that ***(i)*** the computational domain is discretized using a logarithmic mesh generated with the *numpy* library, employing linear interpolation polynomials, ***(ii)*** the backward Euler method is applied for time discretization and ***(iii)*** the Portable, Extensible Toolkit for Scientific Computation (PETSc) [11] is integrated into the implementation for solving the resulting linear systems. The generalized minimal residual method (GMRES) uses an incomplete LU factorization $(ILU(0))$ as the preconditioner.

The numerical test cases examined in this study cover four fundamental scenarios of crystal population dynamics, including pure growth (PG), simultaneous growth and aggregation (GA), simultaneous growth and nucleation (GN), and simultaneous growth, aggregation, and nucleation (GAN). For this analysis, we assume a constant growth rate $g(x,t) = g_0$ and a constant size-independent aggregation kernel $\beta(x,u,t) = \beta_0$. To ensure fair comparison between the Petrov–Galerkin methods, we note that for cases involving:

- pure growth and simultaneous growth and nucleation: the SUPG and GLS formulations become mathematically equivalent ($p_{SUPG}^h = p_{GLS}^h$) since the governing equations contain no reaction terms. This equivalence arises because the problem operator $\mathcal{L}(\cdot)$ reduces to the advective derivative in the absence of reactive or diffusive terms;

- the presence of a diffusion term were present in Eq. (1) would lead to fundamental differences between SUPG and GLS formulations, starting from interpolation functions of second or higher order, since the derivatives in the diffusion term vanish for linear approximations;
- the SUPG and GLS formulations yield distinct perturbations ($p^h_{SUPG} \neq p^h_{GLS}$) in cases involving aggregation phenomena, where the death term $\mathcal{A}_D$ introduces a reaction-type contribution. Unlike diffusion-dominated scenarios, this difference persists for all polynomial orders in the approximation space, as the stabilization mechanisms inherently handle the reactive term differently. Indeed, SUPG only accounts for advective effects (streamline diffusion), while GLS incorporates both advection and reaction through the full operator $\mathcal{L}(\cdot)$.

Based on these considerations, we selected the case involving simultaneous growth and aggregation to evaluate the method performance, leveraging the existence of an analytical solution [12] and [13]. For each time step n and mesh node i, we compute the root mean square deviation (RMSD), generating a family of RMSD curves, one per time step. The method yielding the lowest RMSD across the temporal evolution is considered the most accurate. The RMSD is defined by:

$$RMSD(t_n) = \sqrt{\frac{1}{N_e+1}\sum_{i=1}^{N_e+1}\left[f(x_i,t_n) - f^h(x_i,t_n)\right]^2}. \tag{10}$$

5 Numerical experiments

The numerical experiments were conducted considering the following initial distribution $f_0(x)$ and nucleation $\mathcal{N}(x,t)$ functions

$$f_0(x) = \frac{N_0}{x_0}\exp\left(-\frac{x}{x_0}\right); \tag{11}$$

$$\mathcal{N}(x,t) = \frac{\dot{N}_{0n}}{x_{0n}}\exp\left(-\frac{x}{x_{0n}}\right), \quad \forall t \in T, \tag{12}$$

where N_0 and x_0 are the total number of crystals and the mean volume at the onset of the process, $\dot{N}_{0n}$ is the nucleation rate of crystals of all sizes, and x_{0n} is a parameter in the exponentially distributed nucleation rate. The numerical parameters employed in our simulations are presented in Table 2.

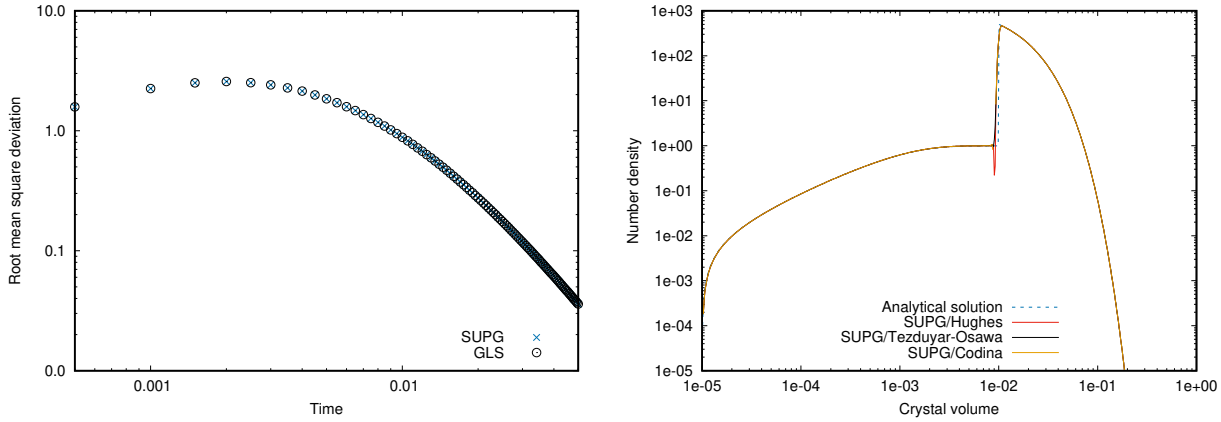
Table 2. Numerical parameters used in computational experiments

Symbol	Meaning [unit]	Value
$x_{\min}$	Smallest crystal volume [u.v]	10^{-5}
$x_{\max}$	Largest crystal volume [u.v]	10
g_0	Growth rate [u.v/u.t]	1
N_0	Total number of crystals at time $t = 0$ [# crystals]	5
x_0	The mean volume of crystals at time $t = 0$ [u.v]	10^{-2}
$\dot{N}_{0n}$	Nucleation rate of crystals of all sizes [# crystals/u.v u.t]	1
x_{0n}	Parameter of the nucleation function [d]	10^{-3}
β_0	Constant aggregation coefficient for scenarios PG/GAN [1/# crystals u.t]	$100/1000$

u.v = unit of volume; u.t = unit of time; d = dimensionless

Both the SUPG and GLS methods were tested using the three stabilization parameters presented in Table 1. To assess their numerical behavior in the case involving simultaneous growth and aggregation, simulations were conducted on a mesh consisting of 900 elements, with a time step of $\Delta t = 5 \times 10^{-4}$ [u.t]. Although the GLS method introduces a perturbation that also affects the reaction term, its performance was found to be nearly equivalent to that of the SUPG method. Fig. 1a shows the RMSD results for both SUPG and GLS methods. Given the similarity in RMSD results for both methods across all stabilization parameters, and to avoid visual clutter in Fig. 1a caused by overlapping curves, we chose to present only the results corresponding to the stabilization parameter proposed in Tezduyar and Osawa [9] for each method.

The GN case was selected to further assess the accuracy of each method. We selected this case to take advantage of the discontinuity, as it provides a suitable scenario for evaluating the behavior of spurious solutions under different stabilization parameters. In this case, $p^h_{SUPG} = p^h_{GLS}$. and since the SUPG method introduces a perturbation that acts exclusively on the convection term, it is slightly less computationally intensive than the GLS



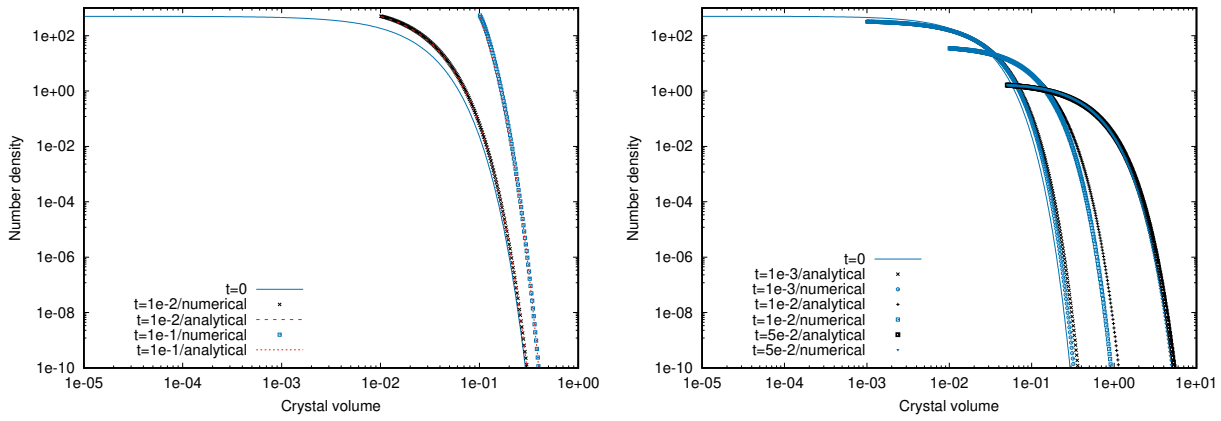
(a) RMSD: simultaneous growth and aggregation

(b) Constant growth with nucleation case at $t = 10^{-2}$

Figure 1. Root mean square deviation and numerical behavior of stabilization parameters

method. Consequently, the SUPG formulation was adopted to evaluate which stabilization parameter achieves the closest agreement with the analytical solution. Fig. 1b presents a comparative analysis between the analytical solution for number density and the numerical SUPG solutions obtained with various stabilization parameters. We observe that the SUPG method using the stabilization parameters proposed by Hughes et al. [7] and Codina [10] leads to oscillations near the discontinuity region, whereas the solution obtained with the parameter introduced by Tezduyar and Osawa [9] demonstrates superior accuracy, maintaining both physical fidelity and agreement with the analytical solution. Therefore, we adopted the SUPG method with the stabilization parameter proposed by Tezduyar and Osawa [9] for all subsequent simulations.

For constant growth, the total number of crystals remains constant since no new particles are generated in the absence of a nucleation process. As a result, the number density curve progressively shifts to the right, reflecting the growth of the crystal population over time, as shown in Fig. 2a. In Fig. 2b, we observe the GA case, where crystals collide and aggregate, forming particles of larger sizes. As a result, the number density decreases over time, as crystals of volume x disappear in accordance with the formation of crystals with greater volume. Note that for constant growth rate scenarios, the number density remais valid $\forall x > g_0 t$. This maintains physical consistency since crystal volumes are inherently defined only $\forall x > 0$; otherwise, solutions extending below $g_0 t$ would violate fundamental physical constraints.



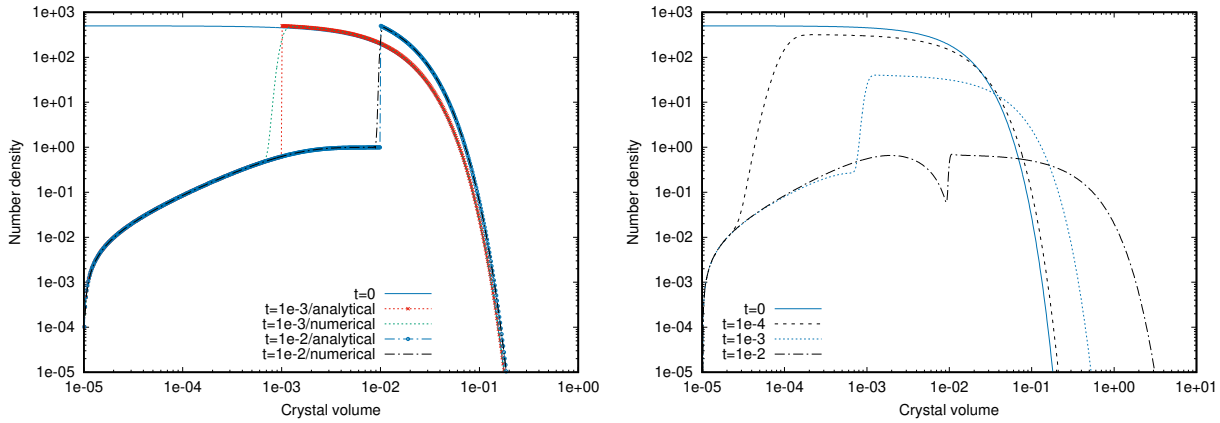
(a) Constant pure growth at different instants

(b) Simultaneous growth and aggregation

Figure 2. Pure growth and simultaneous growth and aggregation cases at different instants

Fig. 3 shows the numerical behavior of the number density function at different times for scenarios GN and GAN. Here, we use $\Delta t = 10^{-5}$ [u.t] to keep accuracy. In Fig. 3a, we observe simultaneous growth with nucleation, where crystals continuously nucleate across the entire range of volumes, from the smallest to the largest. Here, the nucleation function $\mathcal{N}(x,t)$ is such that when $x \to \infty$, then $\mathcal{N}(x,t) \to 0$. As a result, a greater number of crystals with small volumes are nucleated compared to larger ones, while all crystals undergo concurrent growth

over time. Finally, Fig. 3b illustrates the simultaneous occurrence of all phenomena: crystals of various sizes nucleate, aggregate, and grow concurrently. In contrast to the behavior shown in Fig. 3b, the number density decreases over time as a result of the aggregation phenomenon.



(a) Simultaneous growth and nucleation

(b) Simultaneous growth, aggregation and nucleation

Figure 3. Temporal evolution of the number density function comparing scenarios with and without aggregation effects, using a timestep of $\Delta t = 10^{-5}$ [u.t].

6 Conclusions

In this work, the performance of various stabilized finite element methods for solving integro-differential population balance equations was evaluated, considering different stabilization parameters. The root mean square deviation (RMSD) indicates that both methods, under all stabilization parameters, exhibited high similarity in reproducing the expected physical behavior and were in agreement with the analytical results. Therefore, the GA case was selected to identify the method that provides the most accurate approximation. Based on this analysis, we conclude that the SUPG method using the stabilization parameter proposed by Tezduyar and Osawa [9] delivered the best performance. Finally, all cases were run using this selected configuration, and the case involving all phenomena, for which no analytical solution is available, also demonstrated consistent performance aligned with the expected physical behavior.

Acknowledgements. Andrés M. N. Chacón is supported by the *Fundação de Amparo à Pesquisa do Estado do Rio de Janeiro* - FAPERJ, Grant number E-26/201.614/2025. Regina C. Almeida acknowledges the support provided by Brazilian National Council for Scientific and Technological Development (CNPq), Grant number 306588/2022-6.

Authorship statement. The authors hereby confirm that they are the sole liable persons responsible for the authorship of this work and that all material that has been herein included as part of the present paper is either the property (and authorship) of the authors or has the permission of the owner to be included here.

References

[1] M. Bohnet. Fouling of heat transfer surfaces. *Chemical engineering & technology*, vol. 10, n. 1, pp. 113–125, 1987.

[2] K. Shaikh, K. M. S. Newaz, M. N. M. Zubir, K. H. Wong, W. A. Khan, S. Abdullah, M. S. Alam, and L. Sugumaran. A review of recent advancements in the crystallization fouling of heat exchangers. *Journal of Thermal Analysis and Calorimetry*, vol. 148, n. 22, pp. 12369–12392, 2023.

[3] N. Epstein. Thinking about heat transfer fouling: a 5× 5 matrix. *Heat transfer engineering*, vol. 4, n. 1, pp. 43–56, 1983.

[4] I. Babuška, R. S. Silva, and J. Actor. Break-off model for $CaCO_3$ fouling in heat exchangers. *International Journal of Heat and Mass Transfer*, vol. 116, pp. 104–114, 2018.

[5] C. B. B. Costa, M. R. W. Maciel, and R. Maciel Filho. Considerations on the crystallization modeling: Population balance solution. *Computers & chemical engineering*, vol. 31, n. 3, pp. 206–218, 2007.
[6] A. N. Brooks and T. J. Hughes. Streamline upwind/petrov-galerkin formulations for convection dominated flows with particular emphasis on the incompressible navier-stokes equations. *Computer methods in applied mechanics and engineering*, vol. 32, n. 1-3, pp. 199–259, 1982.
[7] T. J. Hughes, L. P. Franca, and G. M. Hulbert. A new finite element formulation for computational fluid dynamics: Viii. the galerkin/least-squares method for advective-diffusive equations. *Computer methods in applied mechanics and engineering*, vol. 73, n. 2, pp. 173–189, 1989.
[8] D. Ramkrishna and M. R. Singh. Population balance modeling: current status and future prospects. *Annual review of chemical and biomolecular engineering*, vol. 5, n. 1, pp. 123–146, 2014.
[9] T. E. Tezduyar and Y. Osawa. Finite element stabilization parameters computed from element matrices and vectors. *Computer Methods in Applied Mechanics and Engineering*, vol. 190, n. 3-4, pp. 411–430, 2000.
[10] R. Codina. On stabilized finite element methods for linear systems of convection–diffusion-reaction equations. *Computer Methods in Applied Mechanics and Engineering*, vol. 188, n. 1-3, pp. 61–82, 2000.
[11] L. D. Dalcin, R. R. Paz, P. A. Kler, and A. Cosimo. Parallel distributed computing using python. *Advances in Water Resources*, vol. 34, n. 9, pp. 1124 – 1139. New Computational Methods and Software Tools, 2011.
[12] S. Qamar and G. Warnecke. Numerical solution of population balance equations for nucleation, growth and aggregation processes. *Computers & Chemical Engineering*, vol. 31, n. 12, pp. 1576–1589, 2007.
[13] S. Kumar and D. Ramkrishna. On the solution of population balance equations by discretization—iii. nucleation, growth and aggregation of particles. *Chemical Engineering Science*, vol. 52, n. 24, pp. 4659–4679, 1997.